PCCP

ARTICLE TYPE

Cite this: DOI: 00.0000/xxxxxxxxxx

Supplementary Information for: A multiscale approach for electronic transport simulation on carbon nanostructures in aqueous solvent

Ernane de Freitas Martins,[a‡] Ralph Hendrik Scheicher,[b] Alexandre Reily Rocha[a] and Gustavo Troiano Feliciano[c*]

Received Date
Accepted Date

DOI: 00.0000/xxxxxxxxxx

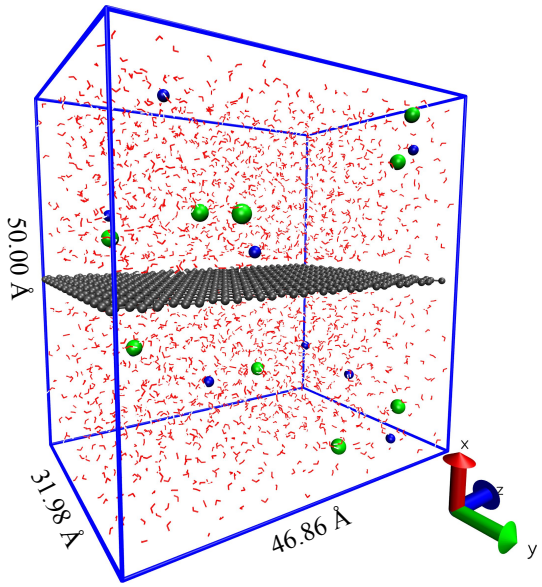

Fig. 1 Simulation box used to study graphene with 0.2 M NaCl. The green spheres represent the Cl ions and the blue ones represent the Na ions. The box dimensions is the same for all simulated systems in the NPT ensemble.

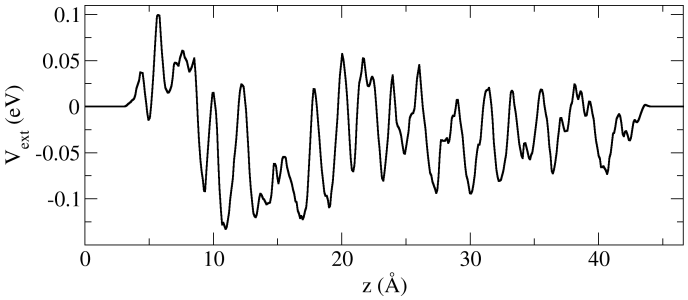

Fig. 2 Electrostatic potential example averaged in the xy plane for frame 17300 of the non-polarized pure water system. The potential is brought to zero at the extremes (electrodes region), and the variations observed are due to the presence of negative (O atoms) and positive (H atoms) close to the graphene sheet.

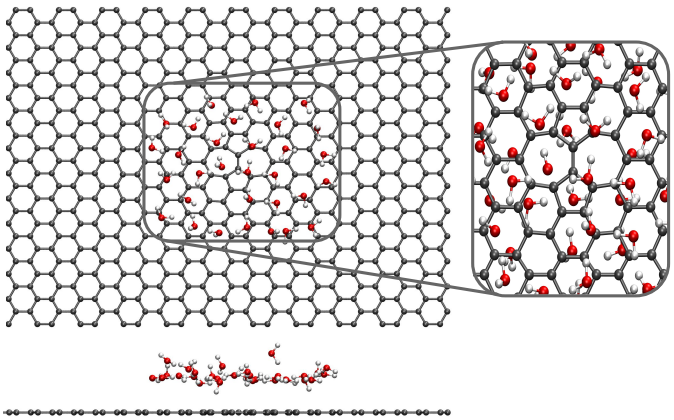

Fig. 3 Top view with a zoom at the defect region and side view for a typical frame for water molecules close to the Stone Wales defect. The square around the defect has dimensions of 14 x 17 Å^2.

[a]*Institute of Theoretical Physics, São Paulo State University (UNESP), São Paulo, Brazil*
[b]*Division of Materials Theory, Department of Physics and Astronomy, Uppsala University, SE-751 20 Uppsala, Sweden*
[c]*Institute of Chemistry, São Paulo State University (UNESP), Araraquara, Brazil*
‡Current address: Catalan Institute of Nanoscience and Nanotechnology (ICN2), CSIC and BIST, Campus UAB, Bellaterra, 08193 Barcelona, Spain and Advanced Manufacturing and Fabrication, School of Engineering, RMIT University, Melbourne, VIC 3000, Australia
∗ Corresponding author. Tel: +55 16 3301-9869. E-mail: gtroiano@iq.unesp.br

1 Convergence Analysis

Through long molecular dynamics (MD) calculations, we have, in principle, a sampling of all the phase space of the system. To

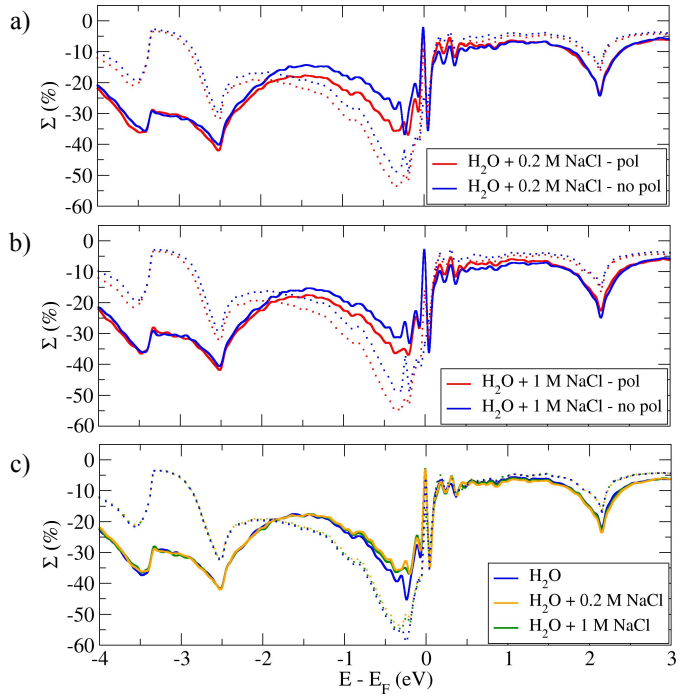

Fig. 4 Further calculations of electronic transport in graphene. Difference between solvated and dry electronic transport curves (Σ) for polarized and non-polarized cases with (a) 0.2 M NaCl and (b) 1 M NaCl, and (c) difference between solvated and dry cases for pure water, 0.2 M NaCl and 1 M NaCl polarized systems.

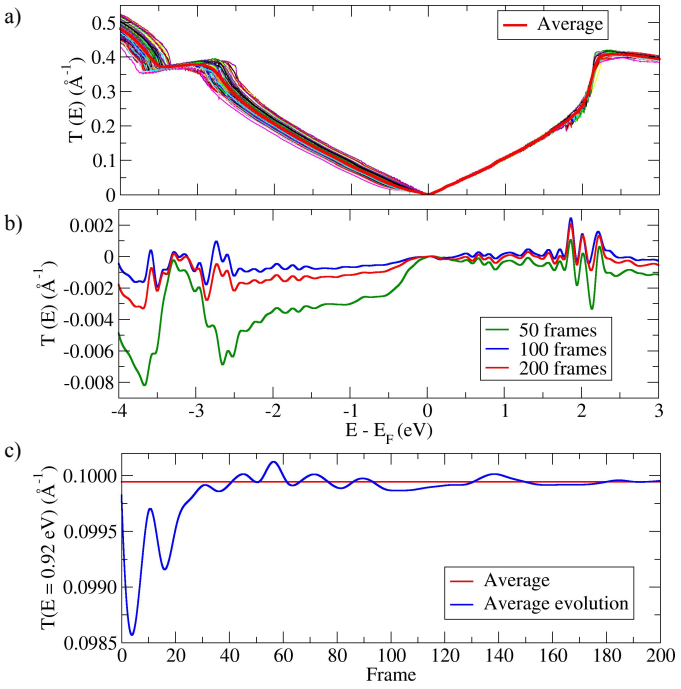

Fig. 5 Convergence analysis for electronic transport calculations using the non-polarized graphene in water with 0.2 M NaCl as an example. In (a), all the 200 calculated electronic transport curves and its the averaged curve are shown. In (b), the difference in the averages over different amounts of frames using the case calculated using 20 frames as reference is presented. In (c), it is shown the evolution of the average transmission for E = 0.92 eV (Fermi Energy moved to zero) as a function of the number of frames.

describe a property over these structures, like electronic transport calculations, we should consider all these sampled structures, or as much as possible, since all of them are possible to be accessed. However, apart from the size of these systems, applying the methodology used in this paper for all the frames of a MD calculation is very expensive, and can become unpractical.

Based on that, we can make a convergence analysis to show the number of structures needed to converge the electronic transport calculation. Therefore, a reduced number of structures can be used to represent all possible structures accessed in the MD sampling. In this manner, we chose the system without polarization for 0.2 M NaCl to perform the convergence analysis, as shown in Figure 5.

Figure 5-a present the electronic transport curves for all 200 frames in the same graph. The thicker red curve is the average over all those curves. As we can see, for energies lower than the Fermi Energy, the broadening is more significant than the case of energies above the Fermi Energy.

Figure 5-b presents the differences in the averages over 50, 100, and all the 200 frames, using the average over 20 frames as a reference. The frames were also chosen equally spaced, and as can be seen in Figure 5-b, the differences are very small compared to the values shown in Figure 5-a. Moreover, the average difference for the cases using 100 and 200 frames are very close. In this way, 100 frames, or even 50 since the difference in average is no so large, would be enough to represent all frames. Besides that, we used 200 frames in all cases presented in the paper to guarantee a good sampling and convergence.

Finally, Figure 5-c presents the evolution of the average for all the 200 frames. The transmission for 0.92 eV was extracted from each frame and averaged up to that point (from 2 to 200 frames). The red curve in the figure is the averaged transmission for that energy over all the 200 frames. The energy of 0.92 eV was chosen arbitrarily since all the transport presented in Figure 5-a are only shifts compared to the average. Thus, in Figure 5-c we analyze a specific value of energy to evaluate its convergence.

In the first 80 frames, we can see a more significant fluctuation of the averaged transmission for that energy. After 80 frames and onward, the fluctuation decreases, and the average evolution tends to the average over all 200 frames. In this way, all plots shown Figure 5 demonstrates that 200 frames are enough to converge the electronic transport of the system.

2 QM/MM partition criteria

One way of investigating how many water molecules make up the first solvation shell of graphene is through the number density analysis on the MD snapshots. In this manner, Figure 6 shows the number density of oxygen atoms as a function of the box size in the x direction, which is perpendicular to the graphene plane. The first peak appears between 2.5 and 3 Å, and the first valley appears around 5 Å.

Figure 6 indicates that the first layer of water is highly organized and also indicates the formation of a second solvation shell. In this way, the Figure presented in the paper for the OH tilt an-

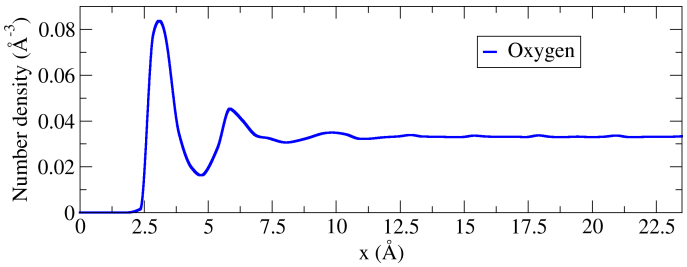

Fig. 6 Number density for oxygen atoms. Only the half part of the simulation box is shown, for clarity, and graphene is placed at x = 0 Å in the plot, in the middle of the box.

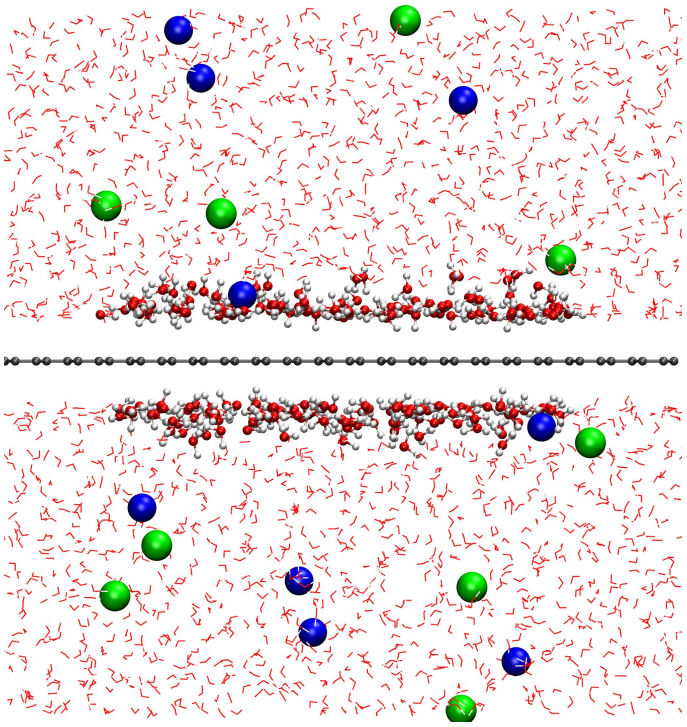

Fig. 7 Side view of a typical frame for the non-polarized graphene in water with 0.2M NaCl. The graphene and water in "ball and sticks" representation make up the QM region whereas the water in "line" representation and the NaCl (green and blue "ball" representation) make up the MM region.

gle in different solvation shells combined with Figure 6 shows that 5 Å is enough to include all water molecules which have its structures altered by the interaction with graphene. The other molecules are bulk-like water, and it is not needed to include them in the QM region for our analysis.

Thus, a typical frame for the case non-polarized graphene in water with of 0.2M of NaCl with the new QM/MM partition is shown in Figure 7. The results regarding the electronic transport calculations for this new partition were presented in the paper, together with the cases of pure water and 1M NaCl. The "ball and sticks" water molecules shown in Figure 7 are chosen as we discussed before, using a distance criterion of 5 Å.

3 The case of non-fixed graphene

All calculations presented in the paper were carried out freezing the graphene coordinates. Here we present the case of free graphene, thus not fixing its coordinates. Figure 8 shows a typical snapshot for free graphene and the electronic transport calculations in pure water in a vacuum, i.e., not taking into account the calculated external potentials (effect of solvent). Therefore, both curves shown in Figure 8 are averaged over the selected MD snapshots.

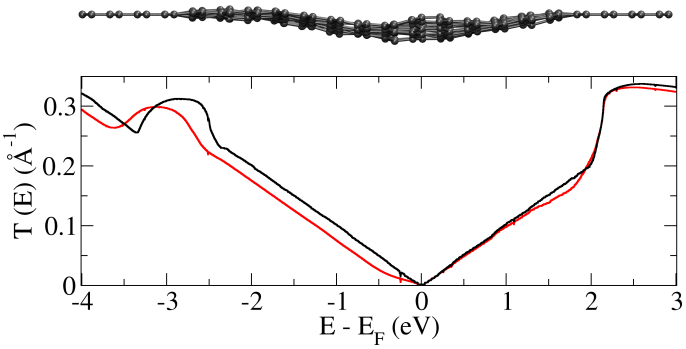

Fig. 8 Side view for a typical snapshot of free graphene (upper panel) and comparison between the electronic transport calculations in (red line) pure water and in (black line) a vacuum (lower panel).

As in the first case presented in the paper (Figure 4-a), the transmittance in a liquid is lower than the transmittance in a vacuum, and we observe that behavior below the Fermi Level in both cases. When allowing the graphene atoms to move, the main effect on the electronic transport can be observed for energies around -3 eV, comparing Figures 8 and Figure 4-a in the paper. In this region, the transmittance for the case in a solution can reach values larger than the ones in a vacuum, which was not observed before. Thus, the solvent effects in the electronic transport properties of graphene are the same if we model it with free or fixed coordinates.

4 Final analysis and summary

As a final analysis, we can plot all the electronic transport calculations for non-polarized pure water systems in the same graphic. Then, Figure 9 summarizes all the electronic transport calculations for these systems: dry pristine graphene (filled black curve), dry Stone Wales (SW) graphene (doted black curve), pristine graphene in pure water (blue curve), pristine graphene with the first solvation shell of water in the QM part (pink curve), and finally SW graphene in pure water (red curve). **Finally, one case where we consider a non neutral graphene sheet is presented as a proof of concept (green curve).**

The first aspect we can see in Figure 9 is that the dry pristine graphene has the largest transmittance (filled black curve), which is expected when we consider a perfect graphene sheet since the scattering of the electrons will be small compared to the other setups in the same plot. As can be also seen in Figure 9, the SW graphene case in pure water (red curve) presents the smallest transmittance for a wide range of energy, showing that the

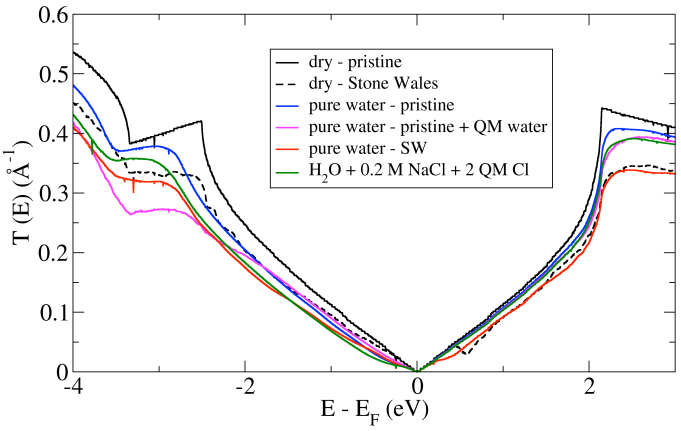

Fig. 9 Summarized comparison of the electronic transport calculations for all pure water non-polarized systems**, and for the case where we consider a non neutral graphene sheet.**

presence of defects plays the role of increasing the scattering of electrons.

As for the case where we consider a different QM/MM partition, one can observe that from -2 *eV* to 2 *eV* the transmittance for both QM/MM partitions are quite similar, as can be seen by comparing the pink and blue curves. However, out of that energy range, we observe that the case that includes explicit water molecules presents a small transmittance, thus a larger scattering, especially for energies below -2 *eV*. For this range of energy, the transmittance for pristine graphene with QM water molecules (pink curve) is smaller than the one for SW graphene in pure water (red curve), showing that the inclusion of water molecules scatters more the electrons compared to the inclusion of SW defect.

We also performed one case where graphene carries a net charge as a proof of concept. For that, we selected the system containing 0.2 M of Na Cl to test the case with a charged graphene sheet in the classical molecular dynamics calculations. We added a +2 charge in the graphene sheet equally distributed over all Carbon atoms. To do so, we needed to add an imbalance of Cl ions to keep charge neutrality, totalizing 11 Cl and 9 Na ions. We then performed a 20 ns NVT simulation. After that, we selected 50 snapshots equally spaced in time, placing the 2 Cl ions nearest to the graphene sheet in the QM region, keeping the charge neutrality between the QM/MM regions - the total charge of the QM subsystem was set to zero in order to prevent spurious charge interactions between periodic images. We choose a reduced number of snapshots due to the cost of these simulations, but that amount is enough to produce a converged average curve, as we showed in Figure 5. We then computed the MM potentials, the single-point energy DFT calculations, and finally, the electronic transport calculations. All simulations were performed with the same parameters used in all the other simulations presented in the main manuscript, and the resulting average transmission curve is presented in the green curve of Figure 9.

The green curve in Figure 9 shows that the transmission is smaller than both dry (black curve) and solvated (blue curve) graphene for energies below the Fermi energy. That result evinces an enhanced doping effect for the case where we include 2 Cl atoms in the QM subsystem. That is expected since graphene will become positively charged whereas the Cl atoms will become negatively charged during the DFT simulations. Please observe that the +2 net charge is added in the MD step and for the DFT (QM/MM) step that charge is naturally acquired by the atoms. The charge acquired by graphene can be evaluated by the plot shown in Figure 10, where we show a histogram of the total Mullikan net charge from our 50 QM/MM calculations. The carrier density estimation obtained by dividing the Mullikan net charge by the graphene area is shown on the bottom x-axis.

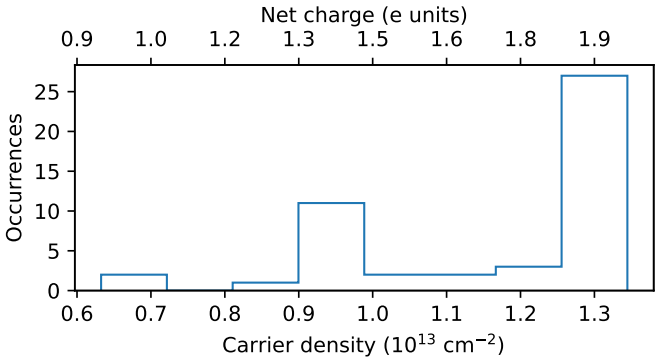

Fig. 10 Carrier density/net charge histogram over the 50 QM/MM calculations for non-polarized graphene in water with 0.2M NaCl with an imbalance of 2 Cl atoms.

As we can observe, many snapshots present a carrier density of around 1.3 x 10^{13} cm^{-2}, similar to the charge doping observed in graphene for adsorbate surface doping[1]. In this way, when we consider a charged graphene, what we observe is a doping effect due to the presence of Cl ions close to the sheet. As we mentioned, that is required to consider a non neutral graphene sheet in our methodology.

Notes and references

1 Y. Yin, Z. Cheng, L. Wang, K. Jin and W. Wang, *Scientific Reports*, 2014, **4**, 5758.